



**Reaching Ultra-High Peak Characteristics  
in Relativistic Thomson Backscattering**

I.V. Pogorelsky<sup>a</sup>, I. Ben-Zvi<sup>a</sup>, T. Hirose<sup>b</sup>, S. Kashiwagi<sup>c</sup>, V. Yakimenko<sup>a</sup>, K. Kusche<sup>a</sup>,  
P. Siddons<sup>a</sup>, T. Kumita<sup>b</sup>, Y. Kamiya<sup>b</sup>, T. Omori<sup>d</sup>, J. Urakawa<sup>d</sup>, M. Washio<sup>c</sup>,  
K. Yokoya<sup>a</sup>, F. Zhou<sup>e</sup>, D. Cline<sup>e</sup>, A. Zigler<sup>f</sup>, B. Greenberg<sup>f</sup>, D. Kaganovich<sup>g</sup>,  
I Pavlichine<sup>h</sup> and I. Meshkovsky<sup>h</sup>

<sup>a</sup> Accelerator Test Facility, Brookhaven National Laboratory, 820, Upton, NY 11973, USA

<sup>b</sup> Physics Department, Tokyo Metropolitan University, Japan

<sup>c</sup> Waseda University, Japan

<sup>d</sup> KEK, Japan

<sup>e</sup> University of California, Los Angeles, Los Angeles, CA 90024, USA

<sup>f</sup> Hebrew University, Jerusalem, Israel

<sup>g</sup> Optoel-Intex Co, St. Petersburg, Russia

October 2002

**CENTER FOR ACCELERATOR PHYSICS**

**BROOKHAVEN NATIONAL LABORATORY**

**BROOKHAVEN SCIENCE ASSOCIATES**

Under Contract No. DE-AC02-98CH10886 with the  
**UNITED STATES DEPARTMENT OF ENERGY**

#### DISCLAIMER

This report was prepared as an account of work sponsored by an agency of the United States Government. Neither the United States Government nor any agency thereof, nor any of their employees, nor any of their contractors, subcontractors, or their employees, makes any warranty, express or implied, or assumes any legal liability or responsibility for the accuracy, completeness, or usefulness of any information, apparatus, product, or process disclosed, or represents that its use would not infringe privately owned rights. Reference herein to any specific commercial product, process, or service by trade name, trademark, manufacturer, or otherwise, does not necessarily constitute or imply its endorsement, recommendation, or favoring by the United States Government or any agency, contractor or subcontractor thereof. The views and opinions of authors expressed herein do not necessarily state or reflect those of the United States Government or any agency, contractor or subcontractor thereof.

# Reaching Ultra-High Peak Characteristics in Relativistic Thomson Backscattering

I.V. Pogorelsky<sup>a</sup>, I. Ben-Zvi<sup>a</sup>, T. Hirose<sup>b</sup>, S. Kashiwagi<sup>c</sup>, V. Yakimenko<sup>a</sup>, K. Kusche<sup>a</sup>,  
P. Siddons<sup>a</sup>, T. Kumita<sup>b</sup>, Y. Kamiya<sup>b</sup>, T. Omori<sup>d</sup>, J. Urakawa<sup>d</sup>, M. Washio<sup>c</sup>,  
K. Yokoya<sup>d</sup>, F. Zhou<sup>e</sup>, D. Cline<sup>e</sup>, A. Zigler<sup>f</sup>, B. Greenberg<sup>f</sup>, D. Kaganovich<sup>f</sup>,  
I Pavlichine<sup>g</sup> and I. Meshkovsky<sup>g</sup>

<sup>a</sup> Accelerator Test Facility, Brookhaven National Laboratory, 820, Upton, NY 11973, USA

<sup>b</sup> Physics Department, Tokyo Metropolitan University, Japan

<sup>c</sup> Waseda University, Japan

<sup>d</sup> KEK, Japan

<sup>e</sup> University of California, Los Angeles, Los Angeles, CA 90024, USA

<sup>f</sup> Hebrew University, Jerusalem, Israel

<sup>g</sup> Optoel-Intex Co, St. Petersburg, Russia

**Abstract.** We observed the record  $1.7 \times 10^8$  x-ray photons/pulse yield generated via relativistic Thomson scattering between the 14 GW CO<sub>2</sub> laser and 60 MeV electron beam.

## 1. INTRODUCTION

The concept of x-ray laser synchrotron sources (LSS) [1] based on Thomson scattering between laser photons and relativistic electrons leads to future femtosecond light-source facilities fit to multidisciplinary research in ultra-fast structural dynamics [2]. Enticed by these prospects, the Brookhaven Accelerator Test Facility (ATF) embarked into development of the LSS based on a combination of a photocathode RF linac and a picosecond CO<sub>2</sub> laser [3,4]. Later the study evolved into international collaboration. Participating institutions are listed in the head of this report.

Selection of a photocathode RF linac and a picosecond CO<sub>2</sub> laser as principal components of the LSS is based on a systematic approach to optimize the LSS towards maximum photon yield. To compare with other previously demonstrated and proposed LSS (driven by ultra-fast solid state lasers) [5-7], the CO<sub>2</sub> laser driver offers certain advantages [3,4,8]. In particular, the CO<sub>2</sub> laser beam, having wavelength  $\lambda=10 \mu\text{m}$ , carries 10 times more photons than a solid state laser ( $\lambda=1 \mu\text{m}$ ) of the same power. This implies a proportionally higher x-ray yield for the LSS.

Two basic configurations are typically used in Thomson scattering: a 90-degree geometry where the e-beam and laser beam are orthogonal to each other, and a 180-degree geometry where the beams collide head-on to each other. In the 90<sup>0</sup> geometry the x-ray pulse length is defined not just by the laser but by passage across the electron and laser focus that is about 300 fs at the typical rms beam size  $\sigma \approx 50 \mu\text{m}$ . In the 180<sup>0</sup> configuration, the x-ray pulse duration is defined primarily by the electron bunch length  $\tau_x = \tau_b + \tau_L / 4\gamma^2$ , where  $\tau_b$  is the electron bunch length,  $\tau_L$  is the laser pulse length, and  $\gamma$  is the electron Lorentz factor. With the 200 fs electron bunches demonstrated from the RF linac [9] and the recent proposal on chirped bunch compression to 10-20 fs [10], the 180<sup>0</sup> geometry promises the absolutely shortest x-ray pulses.

In designing a high-yield LSS, we choose backscattering (180<sup>0</sup>) also as the most energy efficient interaction geometry. The time interval where the counter-propagating focused laser and electron beams stay in interaction is normally  $\pi r_L / \lambda$  times (where  $r_L$  is the laser beam radius)

longer than in the  $90^\circ$  geometry prompting correspondingly higher numbers of scattered photons. To obtain this ratio, we take a proportion between the Rayleigh range that defines the interaction length in the backscattering configuration to the laser beam radius that is important for the  $90^\circ$  configuration. Note that the  $180^\circ$  LSS is capable of producing femtosecond x-ray pulses using picosecond and even nanosecond laser pulses (for nanosecond pulses, channeling is required [11]).

In the present paper, we describe results of the proof-of-principle test of the  $\text{CO}_2$  LSS on the picosecond time scale. We used the ATF 14 GW, 180 ps, linearly polarized  $\text{CO}_2$  laser and the 3.5 ps, 0.5 nC, 60 MeV, low emittance  $\epsilon_n=2$  mm mrad electron beam and demonstrated an x-ray yield of  $1.7 \times 10^8$  photon/pulse,  $5 \times 10^{19}$  photon/sec, peaked at  $1.8 \text{ \AA}$ .

## 2. DESCRIPTION OF THE EXPERIMENT AND RESULTS

The principle diagram of the  $\text{CO}_2$  LSS experiment is shown in Fig. 1. Electron beam, produced by the photocathode RF gun and accelerated to 60 MeV ( $\gamma=120$ ) in two linac sections, is focused in the middle of the Thomson interaction cell using upstream quadrupole magnets. Typical electron beam parameters in the interaction point are: bunch charge 0.5 nC, energy spread 0.15%, normalized emittance  $\epsilon_n=2$  mm mrad, bunch duration 3.5 ps, focus spot size down to  $\sigma_b=35 \mu\text{m}$ . Steering coils allow transverse adjustment of the e-beam position inside the interaction cell. Detailed description of the high-brightness ATF linac, beamlines and electron diagnostics can be found elsewhere [12,13].

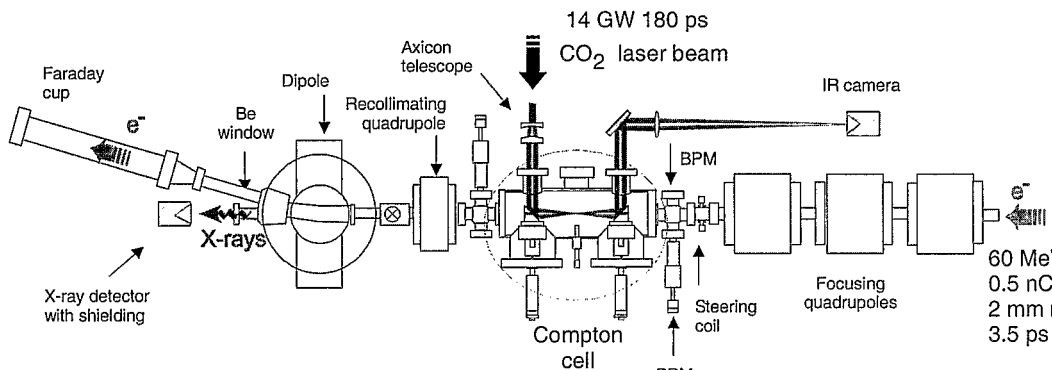


**Figure 1.** Principle diagram of the  $\text{CO}_2$  LSS experiment.

The 5 J, 180 ps pulses generated by the ATF  $\text{CO}_2$  laser [14] are sent to head-on collision ( $180^\circ$  interaction geometry) with the e-beam. In order to produce a tight focus of the  $\text{CO}_2$  laser beam in this geometry, a short focal length optical element (in our case, a copper parabolic mirror with  $F=150$  mm) needs to be placed in the path of the e-beam. Naturally, the mirror has a hole (5 mm in diameter) drilled along the e-beam axis. This hole transmits the backscattered x-rays as well. To avoid laser energy losses and material ablation at the hole edge, we telescope the initially Gaussian laser beam into an annular shaped beam using a pair of ZnSe axicon lenses. Anti-reflection coated ZnSe windows served to introduce the laser beam into the vacuum interaction cell and to extract the spent beam to diagnostics. A mirror mount remotely controlled with stepper motors permitted two-axis tilt of the focusing mirror for precision positioning of the laser focus at the interaction point. The spent laser beam has been extracted from the vacuum cell and recollimated onto an optical diagnostic using a similar parabolic mirror with a hole.

The Thomson scattered x-rays, diverging within a cone of  $\theta = 1/\gamma = 8$  mrad, are detected with the 20 mm aperture Si diode placed outside the vacuum beamline 140 cm downstream from the interaction point. On the way to the detector, the x-ray beam propagates a total distance of 120 cm inside the vacuum beamline, exits through a 250  $\mu\text{m}$  thick Be window and propagates another 20 cm in the air. The electron beam is separated from the x-rays by the bending dipole magnet and is sent to the beam stop. A lead hutch screened the detector from the background noise.

Sizes of the laser and electron beams at the interaction point are evaluated from transmission through the 150  $\mu\text{m}$  pinhole target. Typical transmission of the laser (electron) beam is measured to be 30% (90%) corresponding to the beam size of  $\sigma_L = 60 \mu\text{m}$  ( $\sigma_e = 35 \mu\text{m}$ ).

When the laser and electron beams are aligned and synchronized, we observe Thomson x-ray signal on the Si detector that corresponds to energy deposition of  $1.4 \times 10^{11}$  eV. Based on computer simulation using code CAIN [15] this number is equivalent to  $2.5 \times 10^7$  photons/pulse.

Fig. 2 shows simulated x-ray energy spectrum at the position of the detector. Low energy x-rays are attenuated in the Be window and air, and 15% of photons reach the Si detector. Based on this, we calculate  $1.7 \times 10^8$  photons/pulse produced at the interaction point. Since pulse duration of the x-ray is equal to the electron bunch length (3.5 ps), peak photon density is estimated to be  $5 \times 10^{19}$  photons/second.

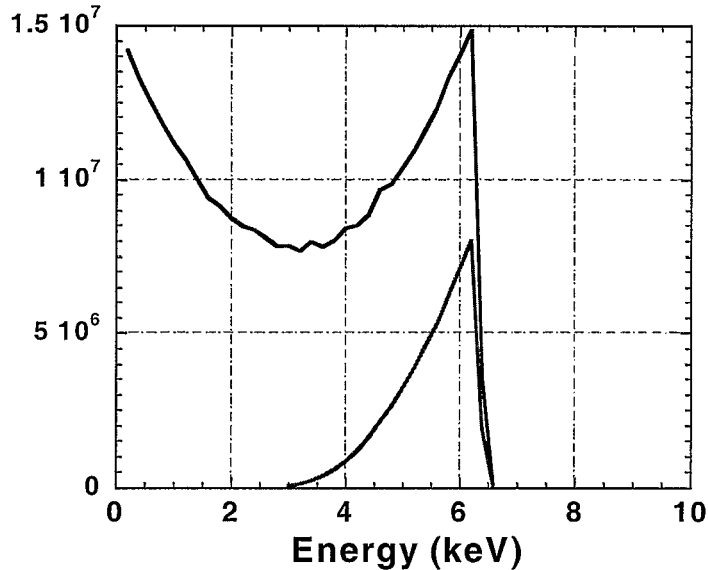


**Figure 2:** X-ray energy spectra simulated by CAIN. The blue line shows the spectrum of all photons generated at the interaction point ( $3.4 \times 10^8$  photons per pulse), while the red line shows photons reach the detector ( $5.0 \times 10^7$  photons,  $2.8 \times 10^{11}$  eV per pulse).

**Table 1** ATF CO<sub>2</sub> LSS experimental results

PARAMETER	VALUE
CO <sub>2</sub> LASER	
Pulse Length [ps]	180
Pulse Energy [J]	3
Peak Power [GW]	14
RMS Radius at Focus [ $\mu\text{m}$ ]	60
Waist Length [mm]	10
ELECTRON BEAM	
Electron Energy [MeV]	60
Bunch Duration FWHM [ps]	3.5
Bunch Charge [nC]	0.5
Normalized Emittance [mm mrad]	2
Momentum Spread [%]	0.15
RMS Radius at Focus [ $\mu\text{m}$ ]	32
X-RAYS	
Peak Wavelength [ $\text{\AA}$ ]	1.8
Pulse Duration [ps]	3.5
Photons per Pulse (total spectrum)	$1.7 \times 10^8$
Photons per Second (total spectrum)	$5 \times 10^{19}$

### 3. DISCUSSION ON SPECTRAL BRIGHTNESS

An important characteristic of the LSS for potential applications is the spectral brightness. The backscattered photons are generated within a cone with a solid angle  $\Omega = 2\pi/\gamma^2$ . Ideally, for every particular observation angle, the radiation spectrum is sharply peaked around its local frequency.

Note that only an infinitely long wave may be ideally monochromatic and well defined upon the scattering angle. In reality, the fractional bandwidth of the electron's radiation depends upon the total number of laser wavelengths  $N$  measured over the electron-laser interaction distance:

$$\Delta\omega'_x/\omega_x = 1/N. \quad (1)$$

Assuming the effective interaction distance is equal to two laser Rayleigh lengths  $2z_0$ , where

$$z_0 = 4\pi\sigma_L^2/\lambda, \quad (2)$$

the time portion of the laser pulse that actually participates in the interaction with the electron bunch is  $4z_0/c$ . Taking the experimentally measured laser beam radius  $\sigma_L=60 \mu\text{m}$ , we obtain  $z_0=5 \text{ mm}$ . Thus,  $4z_0/c=60 \text{ ps}$  that is 2000 laser wavelengths and results in  $\Delta\omega'_x/\omega_x=0.05\%$ .

It also evident from the equation for the fundamental Thomson frequency  $\omega_x^{\text{max}} = 4\gamma^2\omega_L$  that a bandwidth of the scattered x-rays is directly related to the momentum spread or "temperature" of the e-beam as

$$\Delta\omega''_x/\omega_x = 2\Delta\gamma/\gamma. \quad (3)$$

For the ATF e-beam, the temperature smearing in the x-ray spectrum is 0.3%.

The finite divergence of the electron beam at the interaction point also disperses the angular spectrum of the originated x-rays. The e-beam divergence is equal to  $\alpha = \sqrt{\frac{\varepsilon_n}{\gamma\beta}} = \frac{\varepsilon_n}{\gamma\sigma_b}$  and is approximately 0.5 mrad for the parameters of the present experiment. This results in 0.4% spectrum smearing

$$\Delta\omega''_x/\omega_x = (\varepsilon_n/\sigma_b)^2. \quad (4)$$

The combined minimum bandwidth

$$\Delta\omega_x/\omega_x = \sqrt{\Delta\omega'_x{}^2 + \Delta\omega''_x{}^2 + \Delta\omega'''_x{}^2}/\omega_x, \quad (5)$$

for the conditions of the ATF experiment, is equal to 0.5%.

A spectral brightness, which is a cumulative characteristic of the radiation source, is

$$B = \frac{N_x \gamma^2}{4(\pi\sigma_b)^2 \tau_b} = 5 \times 10^{18} \text{ photon/sec /m}^2/\text{rad}^2/0.1\% \text{ bandwidth} \quad (6)$$

for the present ATF experiment conditions.

#### 4. PROSPECTIVE LSS BASED ON THOMSON SCATTERING IN PLASMA CHANNELS

To achieve a high peak intensity and repetition rate, a future LSS type of light source will require a high-power laser and a high brightness electron accelerator both operating at a high repetition rate. In addition, the interacting electron and laser beams need to be tightly focused. The short Rayleigh length of the focused laser beam limits the duration of the interacting pulses to a few picoseconds. Contemporary linear accelerators with photocathode electron injectors meet this requirement. However, a technology of high repetition rate high-average power picosecond lasers is lacking. Another problem associated with the picosecond laser pulses is undesirable nonlinear Thomson scattering occurring when the laser photons are concentrated in a small time-space domain.

In order to abate the technological constraints and achieve a practically feasible intense LSS, we proposed to confine the laser-electron interaction region in a plasma channel, extended over several centimeters [11]. This approach permits the use of nanosecond-long laser pulses instead of picosecond pulses and relieves both aforementioned problems. It evades the nonlinear scattering regime and allows to utilize an existing technology of high-repetition rate TEA (transverse electrical discharge, atmospheric pressure) CO<sub>2</sub> lasers. High repetition rate, multi-kilowatt average power and ~1 ns pulse duration have been demonstrated with such lasers [16].

The number of x-ray photons produced via relativistic Thomson backscattering is given by

$$N_X \approx \frac{8\mathbf{E}_L Q r_e^2 \lambda}{3\hbar e r_L^2}, \quad (7)$$

where  $\mathbf{E}_L$  is the laser pulse energy and  $Q$  is the electron bunch charge. Eq.(7) is derived under the assumption that the laser beam is focused to  $r_L \geq r_b$  and that the electron/photon interaction length extends over the overlap distance defined by the electron and laser pulse duration,

$$L_{\text{int}} \geq \frac{c(\tau_L + \tau_b)}{2}. \quad (8)$$

We would like to have the electron beam confined within the laser beam over the interaction region. The radius  $r_e$  of an electron beam with a normalized emittance  $\varepsilon_n$  and energy  $\gamma$  defines the electron beam waist length  $L_e$

$$L_e \approx \frac{r_e^2 \gamma}{\epsilon_n}. \quad (9)$$

When focused to the same spot, the laser beam usually diverges much faster due to natural diffraction. Thus, we will be interested in a situation when the interaction region (overlap of waists) of counter-propagating focused electron and laser beams is defined primarily by the laser waist length:

$$L_L \approx \frac{\pi^2 r_L^2}{\lambda}. \quad (10)$$

Assuming  $\tau_L \gg \tau_b$  Eqs. (8) and (10) can be reduced to the optimum condition for the laser parameters

$$\frac{\tau_L \lambda}{r_L^2} \approx \frac{2\pi^2}{c}. \quad (11)$$

In order to maximize  $N_x$  value, we shall focus laser to a small  $r_L$ . However, according to Eq.(11)  $\tau_L$  shall be reduced as well. Following this trend and keeping the  $E_L$  high, we ultimately enter a nonlinear regime with the normalized laser strength  $a > 1$ , where

$$a = 0.85 \times 10^{-9} \lambda [\mu\text{m}] I^{1/2} [\text{W}/\text{cm}^2], \quad (12)$$

The nonlinear regime compromises the monochromaticity of the produced Thomson x-rays that will be scattered over many harmonics of the fundamental wavelength

$$\lambda_x = \frac{\lambda(1 + a^2/2)}{4\gamma^2}. \quad (13)$$

Thus, the free space linear Thomson interaction presents certain restrictions for selecting the laser power, pulse duration, and the focal spot size.

The idea of plasma channeling of the laser beam breaks the restriction imposed by Eq. (11) thus opening new possibilities to increase  $N_x$ . Due to confinement of the laser beam over a distance much longer than the Rayleigh length, the laser energy still can be used efficiently even when the pulse length does not increase proportional to  $r_L^2$ , as it is called for by Eq.(11). For the higher energy and proportionally longer laser pulses, the increased number of laser photons interacting with electrons results in higher  $N_x$  without entering the nonlinear regime.

There are a number of proposed schemes and experimental demonstrations for channeling high intensity laser pulses. These include laser guiding in micro-capillary tubes [17,18], plasma channels produced by laser breakdown in the gas [19,20], and by electric discharge in the dielectric tube [21].

Choosing a plasma channel scheme for the ATF LSS we shall apply the following selection rules: First, the channel shall not obscure the produced x-ray cone. This eliminates the use of a narrow capillary. Second, the plasma density needs to be much lower than  $10^{19} \text{ cm}^{-3}$  that is the critical density for the 10- $\mu\text{m}$  beam. This requirement practically rules out methods based on optical breakdown in gas.

Thus, we select the electric discharge scheme that allows to control the plasma density. The laser beam can be confined in the plasma core  $\sim 10$  times smaller than the physical dimensions of the discharge tube. That allows for an interaction between the laser and electron beam and for extraction of the Thomson scattered x-rays without obstruction by the walls.

Until now, all the plasma channel experiments have been performed using picosecond solid state lasers. However, the condition for plasma channeling

$$\Delta n_e [\text{cm}^{-3}] = 10^{20} / r_L^2 [\mu\text{m}], \quad (14)$$

where  $n_e$  is the electron plasma density and  $r_e=2.82\times 10^{-13}$  cm is the classic electron radius, is not sensitive to the laser wavelength. That means that the CO<sub>2</sub> laser may perform as well as a solid state laser that has 10 times smaller wavelength.

In a recent test conducted at the ATF in collaboration with Hebrew University, Jerusalem two-section (ignition and main discharge) polypropylene capillary of the 1 mm inner diameter and 18 mm length was positioned inside a vacuum chamber ( $3\times 10^{-5}$  torr). Up to 14 kV pulsed voltage is applied to the capillary electrodes. The 200 ps, 100 mJ CO<sub>2</sub> laser pulse was focused at the entrance of the capillary with a lens of the 20 cm focal length (F#=12). Another lens imaged the output laser beam with the  $\times 7$  magnification to the Electrophysics pyroelectric video-camera. Intensity profiles are grabbed with the Spiricon laser beam analyzer. Translation of the imaging lens allows observing cross-section of the laser beam at variable depth around the focus inside the vacuum cell.

Intensity distributions shown in Fig. 3a and 3b are obtained in “free space” (capillary retracted). Fig. 3a is taken at the focal point. Fig. 3b is taken at 18 mm distance downstream from the focus. Note that in order to stay within a linear response of the camera and the frame-grabber, images 3a and 3b are obtained with different attenuation. This permits measurement of the beam size that, as we see, expands approximately 6 times in diameter between the observation points that are spaced by  $\sim 6Z_R$  (where  $Z_R$  is the Rayleigh distance)

When we insert a capillary with its entrance tip set at the focal point, establish proper discharge conditions (electrical current and timing) the observed intensity pattern changes from 3b to 3c without refocusing of the imaging lens. Comparison of the image at the plasma channel exit (Fig. 3c) with the distribution in free space at the equivalent distance from the focus (Fig. 3b) demonstrates evident optical guiding effect (optical attenuation has not been changed).

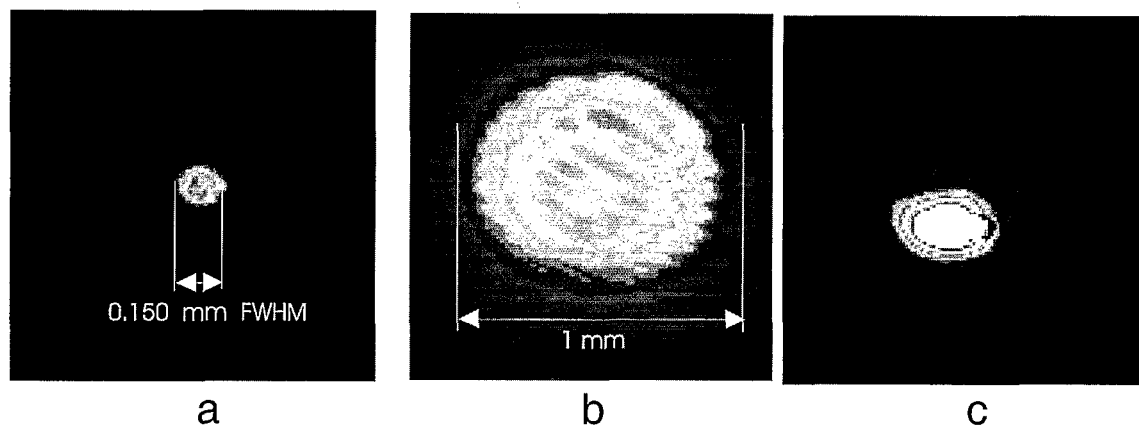


**Figure 3.** CO<sub>2</sub> laser beam transmission through a plasma channel:

a) image of the laser beam at the focal point; b) laser beam image taken 18 mm downstream from the focus in the free space (capillary retracted, attenuation adjusted); c) laser beam image obtained at the exit of the 18 mm long plasma discharge with the capillary entrance placed at the focal point (no attenuation adjustment between b) and c)).

The best channeling condition is obtained at the 12-14 kV voltage applied to the capillary, peak current  $\sim 400$  A, and the laser pulse delayed by  $\sim 120$  ns ( $3/4$  of the current period) relative to the first current peak.

The result shown in Fig. 3 seems to be the first experimental evidence of the 10  $\mu$ m laser beam guiding in a plasma channel. Our observations, being of a special importance for the CO<sub>2</sub> laser applications, simultaneously provide more general confirmation of establishing a plasma channel in the range of  $10^{17}$ - $10^{18}$  cm<sup>-3</sup>. These conditions are of interest for such important

application of guided laser beams (including solid state lasers as well) as laser wakefield acceleration.

## 5. CONCLUSIONS AND FUTURE PLANS

The reported Thomson scattering experiment is a step in development of the high-intensity LSS at the ATF. The obtained agreement between theory and experiment allows extrapolation towards the next stage of the CO<sub>2</sub> LSS, which will utilize 1-TW picosecond CO<sub>2</sub> laser in the same interaction cell. With such a laser, in a combination with the electron bunch compression, the ATF will be in position to demonstrate LSS with the x-ray flux up to 10<sup>22</sup> photon/sec.

This experiment will open an opportunity for study relativistic nonlinear Thomson scattering. With a 1-TW CO<sub>2</sub> laser beam focused to the  $\sigma_L=40$   $\mu\text{m}$  spot  $I_0 = P_L/2\pi\sigma_L^2=10^{16}$  W/cm<sup>2</sup> laser intensity will be attained. According to Eq. (12) this intensity corresponds to the normalized laser strength of  $a\approx 1$ , and the nonlinear Thomson scattering effect comes into view.

Being of a high interest for fundamental QED study, the nonlinear effect is undesirable when designing LSS of a high spectral brightness. To pursue this task, the ATF prepares the Thomson scattering experiment in a plasma channel. The goal of this experiment will be demonstration of the efficient generation of picosecond and femtosecond x-rays using subnanosecond laser pulses at  $a\ll 1$ .

## ACKNOWLEDGMENTS

This study is supported by the U.S. Dept. of Energy under the Contract No. DE-AC02-98CH10886 and Japan/U.S. cooperation in the field of High Energy Physics.

## REFERENCES

- [1] P. Sprangle, A. Ting, E. Esarey, A. Fisher, *J. Appl. Phys.*, **72**, 5032 (1992)
- [2] Recommendations of Basic Energy Sciences Advisory Committee (BESAC) Panel on Novel, Coherent Light Sources <http://www.er.doe.gov/production/bes/BESAC/pubs.html>
- [3] I.V. Pogorelsky, "High-Intensity Laser Synchrotron X-Ray Source", *BNL Preprint*, BNL-62447 (1995)
- [4] I.V. Pogorelsky, I. Ben-Zvi, *Particle Accel. Conf. 97*, Vancouver, B.C., Canada, May 12-16, 1997, <http://www.triumf.ca/pac97/papers/pdf/6V040>
- [5] A. Ting, R. Fischer, A. Fisher, C.I. Moore, B. Hafizi, R. Elton, K. Krushelnick, R. Burris, S. Jakel, K. Evans, J.N. Weaver, P. Sprangle, M. Baine, S. Ride, *Nucl. Instrum. and Methods in Phys. Res. A* **375**, ABS 68 (1996)
- [6] R.W. Schoenlein, W.P. Leemans, A.H. Chin, P. Volbeyn, T.E. Glover, P. Balling, M. Zolotarev, K.-J. Kim, S. Chattopadhyay, C.V. Shank, *Science*, **274**, 236 (1996)
- [7] K. Nakajima, *Proceedings of LASERS'97*, New-Orleans, LA, December 15-19, 1997, STS Press, McLean, VA, 778 (1998)
- [8] I.V. Pogorelsky, *Nucl. Instrum. and Methods in Phys. Res. A* **411**, 172 (1998)

- [9] M. Uesaka, K. Kinoshita, T. Watanabe, T. Ueda, K. Yoshii, H. Harano, J. Sugahara, K. Nakajima, A. Ogata, F. Sakai, H. Dewa, M. Kando, H. Kotaki, S. Kondo, *8<sup>th</sup> Workshop on Advanced Accelerator Concepts*, July 1998, Baltimore, MD, *AIP* **472**, 908 (1999)
- [10] X.J. Wang, "Producing and Measuring Small Electron Bunches", *Proceedings of Particle Accel. Conf. 99*, New York, NY, April 1999
- [11] I.V. Pogorelsky, I. Ben-Zvi, X.J. Wang, T. Hirose, "Femtosecond laser synchrotron sources based on Compton scattering in plasma channels", *Nucl. Instrum. & Methods in Phys. Res. A*, to be published.
- [12] [http://www.nsls.bnl.gov/AccTest/Beam\\_Lines/ATF\\_Beam\\_Lines.htm](http://www.nsls.bnl.gov/AccTest/Beam_Lines/ATF_Beam_Lines.htm)
- [13] X.J. Wang, M. Babzien, K. Batchelor, I. Ben-Zvi, R. Malone, I.V. Pogorelsky, X. Qui, J. Sheehan, J. Skaritka, and T. Srinivasan-Rao, *Nucl. Instrum. and Methods in Phys. Res. A* **375**, 82 (1996)
- [14] I.V. Pogorelsky, J. Fischer, K.P. Kusche, M. Babzien, N.A. Kurnit, L.J. Bigio, R.F. Harrison, and T. Shimada, *IEEE J. of Quant. Electron.* **31**, 556 (1995)
- [15] The manual of code CAIN, <ftp://lcdev.kek.jp/pub/Yokoya/manual-cain21e.ps.zip>
- [16] "Handbook of Molecular Lasers", ed. P.K. Cheo, Marcel Dekker, Inc, New-York, 1987
- [17] Y Jackel, R. Burris, J. Grun, A. Ting, C. Manka, K. Evans, and J. Kosakovskii, *Opt. Lett.* **20** (1995) 1086
- [18] F. Dorchies, J.R. Marques, B. Cros, G. Matthieussent, C. Courtois, T. Velikorossov, P. Audebert, J.P. Geindre, S. Rebibo, G. Hamoniaux, and F. Amiranoff, *Phys. Rev. Lett.* **82** (1998) 4655
- [19] C.D. Durfee III & H.M. Milchberg, *Phys. Rev. Lett.*, **71** (1993) 2409
- [20] E.W. Gaul, S.P. Le Blank, and M.C. Downer, *8<sup>th</sup> Workshop on Advanced Accelerator Concepts*, July 1998, Baltimore, MD, *AIP*, 472 (1999) 377
- [21] Y. Ehrlich, C. Cohen, A. Zigler, J. Krall, P. Sprangle, and E. Esarey, *Phys. Rev. Lett.* **77** (1996) 4186